**EPJ manuscript No.**
(will be inserted by the editor)

# Static and dynamic properties of a dimerized quantum-spin chain

Oliver Fritz[a], Stephen W. Lovesey, and Greg I. Watson

ISIS Facility, Rutherford Appleton Laboratory, Oxfordshire OX11 0QX, United Kingdom

Received: date / Revised version: date

**Abstract.** Various static spin-correlation functions and the weights of the spin excitations, or collective normal-modes, in the van Hove response function, observed in neutron scattering experiments, are calculated as a function of temperature for a model quantum-spin chain. The spins interact through an isotropic Heisenberg exchange that extends to nearest neighbour spins. In our model, spins of magnitude 1/2 form a dimerized chain with alternating exchange interactions. We explore the static and dynamic properties for ferromagnetic and antiferromagnetic exchange interactions. Results for the various properties are shown to be exact in the limit of a large temperature, and we argue the results are very good at small temperatures. The results are also exact in the limit of strong dimerization, *i.e.* non-interacting coupled pairs of spins.

**PACS.** 75.10.Jm Quantized spin models

## 1 Introduction

Recent experimental progress in the investigation of low-lying excitations in one-dimensional spin-1/2 Heisenberg chains has lead to renewed interest in theoretical approaches to model systems. Special attention is given to systems where, either through a spin-Peierls transition, as in the compounds $CuGeO_3$ [1] and $NaV_2O_5$ [2], or through an instrinsic structural asymmetry, as in $CuWO_4$ [3] and $(VO)_2P_2O_7$ [4], the effective intra-chain antiferromagnetic interactions alternate in strength. The materials can show no magnetic order at all ($CuGeO_3$), or, due to inter-chain coupling, long-range antiferromagnetic order ($CuWO_4$). In the absence of magnetic order, the ground state of an isolated chain is well described by a "dimer state", which consists of adjacent pairs of spins coupled into singlets. The dimer state has total spin zero, and a gap to low-lying excitations, because of the energy required to excite a singlet dimer to a triplet. Assuming that such local excitations acquire dispersion by hopping from one dimer to the next, a quantitative account of the well-defined magnon peak observed in neutron-scattering can be given [5,6]. This picture provides an appealing intuitive interpretation of the energy gap at the centre of the Brillouin zone and of the three-fold degeneracy of the excitations, and is exact in the limit of strong dimerization. Conventional spin-wave theory, applied to the paramagnetic state where expectation values of products of spin operators display a full rotational symmetry, cannot readily account for these features.

Neither the spin-wave nor the dimer theory addresses the observed continuum component of the spectrum. This has been interpreted as a two-magnon continuum, or alternatively as a two-soliton continuum [7]. In the dimerized chain, a soliton may be envisioned as a single unpaired spin separating segments of singlet pairs. However, these solitons are subject to a confining effective potential [8], and are always bound in pairs; in this picture, a magnon is a triplet two-soliton bound state. Thus, a two-soliton continuum is possible only in the case of a spin-Peierls chain, and requires a generalization of the model considered here, to include the phonon coupling responsible for spontaneous dimerization. An exception is the limit of a regular (undimerized) chain, such as $KCuF_3$ [9], in which the confining potential vanishes, the solitons unbind and the magnon peak is replaced by a two-soliton continuum. A full understanding of the excitation spectrum of dimerized chains might be revealed with a combination of techniques, including field theories and numerical simulations. A review completed in 1981 of various theories on this subject is found in Ref. [10].

Apart from the dimerized antiferromagnetic chain, one may also consider its ferromagnetic counterpart, and also a "mixed" chain where the couplings alternate in sign as well as magnitude. These cases are less well studied, and existing candidate mixed-chain materials [11,12] are organic compounds, for which crystals suitable for inelastic neutron scattering studies are not available. Past theoretical work on the mixed chain [13] has concentrated on the connection with the $S = 1$ "Haldane gap" system.

The theory presented in this paper treats a dimerized chain of Heisenberg spins $S = 1/2$ with full rotational symmetry and no long-range magnetic order. It can be applied for an arbitrary strength of the dimerization, is, unlike spin-wave theory, correct in the limit of isolated dimers, and the expected results are recovered in the limit

[a] *Present address:* Paul Scherrer Institut, CH-5232 Villigen PSI, Switzerland

of a regular chain. It does not address the continuum part of the spectrum. We show that our results are good in an interval of temperatures of interest in the interpretation of available experimental data. In the limit of an infinite temperature no approximation in the results remains.

In the following section we define the model and describe the method of closing the infinite hierarchy of equations of motion for the spin operators. Thereafter, in sections 3 and 4, one finds our expressions for the static spin-correlation functions, the wave-vector dependent isothermal susceptibility, and the spectral weights of the spin excitations in the van Hove response function observed in neutron scattering experiments. Results for these quantities are found in sections 5 and 6; first a collection of analytic results valid at the two extremes of the temperature and, secondly, extensive results at intermediate temperatures obtained by numerical analysis. Our conclusions are gathered in section 7.

## 2 Model and equations of motion

Quantum-spin operators placed at lattice sites in a chain interact by a Heisenberg exchange mechanism of alternating strength $J$ and $\alpha J$. It is convenient to employ two spin operators, $\mathbf{S}$ and $\mathbf{T}$, of equal magnitude $1/2$, placed at alternate sites in the chain. The Hamiltonian of the dimerized chain is,

$$H = J \sum_l \{\mathbf{S}_l \cdot \mathbf{T}_{l+1} + \alpha\ \mathbf{S}_{l+1} \cdot \mathbf{T}_{l+1}\} \qquad (1)$$

where $l = 0, \pm 1, \cdots$. We will consider also a regular Heisenberg chain whose Hamiltonian is obtained from (1) by setting $\alpha = 1$.

To study the dynamic and static properties of the model we construct the equation of motion for the spin ladder operators $S^+ = S_x + iS_y$, and $T^+$. This is the first equation of an infinite hierarchy of equations for the time development. We close the set of equations at the second level, following a scheme used by Kondo and Yamaji [14] in their study of a regular chain, with $\alpha = 1$.

In constructing the equations one uses $\langle S^\alpha \rangle = 0$, since there is no long-range magnetic order. The model is isotropic in the spin space, so $\langle S^x S^y \rangle = \langle S^y S^z \rangle = \langle S^z S^x \rangle = 0$, and $\langle S_a^\alpha S_b^\alpha \rangle$ is independent of the Cartesian label. Furthermore, $\langle S_a^+ S_b^- \rangle = \langle S_a^- S_b^+ \rangle = 2\langle S_a^z S_b^z \rangle$.

Following a standard prescription [14,15] an expression for the van Hove response function $S(q, \omega)$ is obtained from the approximate equations of motion. This expression contains a number of correlation functions as parameters. Through a Fourier transform over the Brillouin zone these correlation functions are recovered from $S(q, \omega)$, and their values are thus determined by a self-consistency condition. At a temperature large compared to $|J|$, solutions for the correlation functions are found by analytic methods. A numerical method is used to determine the self-consistent solutions at an arbitrary temperature, $T$, which can be checked against the analytic results for $T \gg |J|$. A few analytic results have also been obtained for $T \ll |J|$ and for correlation functions of large spatial index.

## 3 Self-consistent equations

The spin operators $\mathbf{S}$ and $\mathbf{T}$ in (1) have a magnitude $1/2$. In the equations of motion for $S^+$ and $T^+$ we use $(S^+)^2 = (S^-)^2 = 0$ and $(S^z)^2 = 1/4$, and the corresponding identities for $\mathbf{T}$. The equations of motion, obtained by closure at the second level, contain three correlation functions,

$$A_1 = \langle S_l^z T_{l+1}^z \rangle, \quad A_1' = A_{-1} = \langle S_l^z T_l^z \rangle,$$

and

$$A_2 = \langle S_l^z S_{l+1}^z \rangle = \langle T_l^z T_{l+1}^z \rangle. \qquad (2)$$

For $\alpha = 1$ one has $A_1 = A_1'$. A fourth thermodynamic variable, denoted by $\xi$, arises in the mechanism chosen to close the hierarchy of equations, *e.g.*,

$$\begin{aligned} S_l^z S_{l+1}^z T_{l+1}^+ &\approx \xi \langle S_l^z S_{l+1}^z \rangle T_{l+1}^+ \\ &= \xi A_2 T_{l+1}^+ \end{aligned} \qquad (3)$$

The introduction of the variable $\xi$ is essential for the success of our approach. Without this variable, the self-con/-sistency equations would overdefine the correlation functions [16,17].

It is interesting to enquire if the closure of the equations of motion we adopt can be successfully applied to spins $S > 1/2$. We have concluded that closure at the second level, used here, applied to $S > 1/2$ is not robust and entails a larger degree of approximation than found in our case of $S = 1/2$. This view is reached by consideration of terms in the second equation of motion that are zero for $S = 1/2$, *e.g.* $(S^+)^2 S_\alpha$. To reach the same situation for $S = 1$, say, one needs $(S^+)^3 S_\alpha$ and this may first occur at the third level in the hierarchy of equations of motion. So, to achieve the level of approximation we have for $S = 1/2$ with spins of a larger magnitude one must close the hierarchy at the third or higher level.

Our model possesses the obvious property that it is unchanged with the transformation

$$\begin{aligned} &\alpha \to 1/\alpha, \quad J \to \alpha J, \\ &A_1 \to A_1', \quad A_1' \to A_1, \quad A_2 \to A_2. \end{aligned} \qquad (4)$$

This transformation is nothing but an inversion of the lattice around a site and a rescaling of the exchange interactions. We can express this invariance in a more general form by $A_n = A_{-n}'$ for odd integer $n$, and $A_n = A_{-n}$ for even $n$. Note that the index $n$, unlike $l$ in the Hamiltonian (1), counts the total number of bonds between any two spins in the chain. Under the transformation, we find $\xi \to \xi$, cf. (14).

The normal-mode frequencies, and the transcendental equations for $A_1, A_1', A_2$, and $\xi$ are couched in terms of the following quantities. Let $\tilde{A}_n = \xi A_n$, and,

$$\begin{aligned} f &= \frac{1}{2} + 2\alpha \tilde{A}_1' + 2\alpha \tilde{A}_2, \\ g &= \frac{1}{2}\alpha + 2\tilde{A}_1 + 2\tilde{A}_2, \\ \Delta &= 2\alpha(\tilde{A}_1 - \tilde{A}_1'), \end{aligned}$$

and,

$$h = \frac{1}{2}(1+\alpha^2) + 4\alpha\tilde{A}_2. \tag{5}$$

Defining,

$$C = J^2\sqrt{(\alpha g + f)^2 + 2\alpha g f(\cos q - 1) - (\Delta \sin q)^2}, \tag{6}$$

where $q$ is a wave vector in units of the inverse of the distance between two neighbouring $\mathbf{S}$, or $\mathbf{T}$, the four normal-mode frequencies satisfy,

$$\omega_{a,b}^2 = J^2(h + 2\alpha(\tilde{A}_1 + \tilde{A}_1')\cos q) \pm C, \tag{7}$$

Quantities with an index $a$ have to be evaluated using $+C$, and with an index $b$ using $-C$. For $q = 0$ we find $\omega_a \neq 0$, and $\omega_b = 0$. With $\alpha = 1$ the modes cross at $q = \pi$, and the physically relevant mode is $\omega_b$ for $0 < q < \pi$ and $\omega_a$ for $\pi < q < 2\pi$, recovering the result for the regular chain [14] in a doubled Brillouin zone, cf. Figs. 1 and 5. In the limit $\alpha = 0$ one finds $\omega_a = 1$ and $\omega_b = 0$, which follow from the results $A_1' = A_2 = 0$ and $A_1 = -1/4$. For a small value of $\alpha$ we find,

$$\omega_a \simeq J(1 + 2\alpha\tilde{A}_1 \cos q). \tag{8}$$

Next we consider the transcendental equations that follow by calculating any two-spin correlation function from the approximate equations of motion. For a temperature $T$, expressed by $\beta = 1/k_B T$, we find

$$A_n = \frac{1}{4\pi}\int_0^{2\pi}\frac{dq}{C}\{\ \omega_a^{-1}\coth(\beta\omega_a/2)G_a(q) - \omega_b^{-1}\coth(\beta\omega_b/2)G_b(q)\}. \tag{9}$$

For $n = 0, 2, 4, \cdots$, $G_{a,b}(q)$ read

$$\begin{aligned} G_{a,b}(q) = -\ J^3\cos\frac{nq}{2}\ \{&(\pm C/J^2)(A_1 + \alpha A_1') \\ &+ \alpha g(A_1\cos q + \alpha A_1') \\ &+ f(A_1 + \alpha A_1'\cos q)\}, \end{aligned} \tag{10}$$

and for $n = \pm 1, \pm 3, \cdots$, they read

$$\begin{aligned} G_{a,b}(q) = &\ J^3\cos\frac{(n-1)q}{2}\ \{(\pm C/J^2)A_1 \\ &+ f(A_1 + \alpha A_1') + \Delta(A_1\cos q + \alpha A_1')\} \\ &+ J^3\cos\frac{(n+1)q}{2}\ \{(\pm C/J^2)\alpha A_1' \\ &+ \alpha g(A_1 + \alpha A_1') - \Delta(A_1 + \alpha A_1'\cos q)\}, \end{aligned} \tag{11}$$

where, again, indices $a$ and $b$ refer to the sign of $C$. Setting $n = 0$ and $n = 2$ in (10), and $n = \pm 1$ in (11), and thereby recovering $A_0$, $A_2$, $A_1$, and $A_1'$, respectively, we obtain the four equations that are solved self-consistently. For completeness we give $G_{a,b}$ for $A_1$ and $A_1'$ from (11) in a simpler form as

$$\begin{aligned} G_{a,b}^{A_1}(q) = J^3\ \{&(\pm C/J^2)(A_1 + \alpha A_1'\cos q) \\ &+\ \alpha A_1'\Delta\sin^2 q \\ &+\ (A_1 + \alpha A_1')(\alpha g\cos q + f)\} \end{aligned} \tag{12}$$

for $A_1$, and

$$\begin{aligned} G_{a,b}^{A_1'}(q) = J^3\ \{&(\pm C/J^2)(\alpha A_1' + A_1\cos q) \\ &-\ A_1\Delta\sin^2 q \\ &+\ (A_1 + \alpha A_1')(\alpha g + f\cos q)\} \end{aligned} \tag{13}$$

for $A_1'$. One more relation arising from the symmetry of our model is,

$$A_1' - \alpha A_1 + 4\xi\{A_1A_1'(\alpha - 1) + A_2(\alpha A_1' - A_1)\} = 0. \tag{14}$$

We derive this by requiring $A_n$ for $n$ even to be an invariant under the transformation in (4), and we deduce $\xi \to \xi$.

## 4 Observable quantities

The quantity observed by inelastic neutron scattering is the van Hove response, a function of wave vector and frequency,

$$S(q,\omega) = \frac{1}{2\pi}\int_{-\infty}^{\infty} dt\exp(-i\omega t)\times \sum_{m,m'} e^{iq(m'-m)}\langle S_m^+(0)S_{m'}^-(t)\rangle, \tag{15}$$

where $m$ and $m'$ range over every site in the chain. At this point it is important to note that we assume a regular spacing throughout the whole lattice in spite of an alternating exchange interaction. This is in agreement with the very small observed lattice distortion, *e.g.*, in $CuGeO_3$, but not necessarily true for structurally dimerized materials, an example of which is $(VO)_2P_2O_7$. However, only $q$-dependent quantities derived from (15) will be affected by a lattice distortion, and expressions for observable quantities like (16) and (18) will be more complicated. Real-space correlation functions remain unaffected by a lattice distortion.

Since the normal modes are undamped, at the level of approximation we employ, they make contributions to the van Hove response that have a dependence on frequency given by $\delta(\omega \pm \omega_a)$ and $\delta(\omega \pm \omega_b)$. The two $\delta$ functions for the creation events, $\delta(\omega - \omega_{a,b})$ are, apart from the detailed-balance factor $1 + n(\omega)$, accompanied by the spectral-weight functions, given per spin,

$$\mathcal{F}_{a,b}(q) = -J^3\frac{F_{a,b}}{\pm C\omega_{a,b}}(1 - \cos\frac{q}{2}), \tag{16}$$

where

$$\begin{aligned} F_{a,b}(q) = &\ (A_1 + \alpha A_1')(\pm C/J^2 + \alpha g - f - 2f\cos\frac{q}{2}) \\ &+2\Delta(A_1 - \alpha A_1')\cos\frac{q}{2}(1 + \cos\frac{q}{2}) \\ &-2A_1(\alpha g - f)(1 + \cos\frac{q}{2}). \end{aligned} \tag{17}$$

Again, quantities with an index $a$ involve $+C$, quantities with an index $b$ involve $-C$. Finally, we can derive the wave-vector dependent susceptibility $\chi(q)$ per spin from the relation

$$\chi(q) = \int_{-\infty}^{\infty} \frac{d\omega}{\omega} S(q,\omega) = \int_{0}^{\infty} \frac{d\omega}{\omega} \frac{S(q,\omega)}{1+n(\omega)} = \frac{\mathcal{F}_a}{\omega_a} + \frac{\mathcal{F}_b}{\omega_b}. \quad (18)$$

The absence of the usual factor 2 in the right-hand side of the first equality in (18) stems from the fact that we give the susceptibility for correlations $\langle S^z S^z \rangle_q$, which are half the value of $\langle S^+ S^- \rangle_q$, used in (15) and (16).

Results obtained from our model by setting $\alpha = 0$ are easy to derive. It can be shown that the foregoing expressions evaluated for $\alpha = 0$ reproduce those results. Also, setting $\alpha = 1$ we recover all expressions provided for the regular chain as given in [14]. The authors of [14] did not consider the spectral weights (16), the susceptibility (18), nor the dimerized chain.

## 5 Analytic results

First we give the static susceptibility in terms of the correlation functions $A_n$ for arbitrary temperature. We find for $q = 0$,

$$\chi(0) = \frac{-4A_1}{J}(\alpha + 4\tilde{A}_1' + 4\tilde{A}_2) \times \{(\alpha - 4\tilde{A}_1' + 4\tilde{A}_2)(1 - 4\alpha\tilde{A}_1 + 4\alpha\tilde{A}_2) - 64\alpha\tilde{A}_1\tilde{A}_1'\}^{-1}, \quad (19)$$

and for $q = \pi$,

$$\chi(\pi) = \frac{-4A_1(\alpha - 4\tilde{A}_1' + 4\tilde{A}_2)}{J(\alpha - 4\tilde{A}_1' + 4\tilde{A}_2)(1 - 4\alpha\tilde{A}_1 + 4\alpha\tilde{A}_2)}. \quad (20)$$

In the limit $T \gg |J|$, the leading-order terms in an expansion of $A_1, A_1'$ and $A_2$ in terms of $\beta J$ are found to be,

$$A_1 = \frac{-1}{16}\beta J, \quad A_1' = \frac{-\alpha}{16}\beta J,$$

and

$$A_2 = \frac{\alpha}{64}(\beta J)^2. \quad (21)$$

These results are identical to results obtained by an independent calculation of the correlation functions that uses an expansion of $\exp(-\beta H)$, *e.g.*,

$$A_1 = -\beta J \left(\frac{1}{3}S(S+1)\right)^2. \quad (22)$$

For $\xi$ we find from (14) and (21) the value $\xi = 1$ in this limit. Equally, the susceptibility $\chi$ can be derived. It becomes independent of the wave-vector and approaches the well-known result

$$\chi = \frac{1}{4}\beta = \frac{S(S+1)}{3}\beta. \quad (23)$$

On the low temperature-side, analytic results can be derived for $\alpha = 1$, and they coincide with those given in Ref. [14]. For arbitrary $\alpha$, the leading order behaviour for large $n$ can be derived from (9), (10), and (11). In all cases these show at non-zero temperature an exponential decay, with a correlation length which diverges as $T \to 0$. For the pure ferromagnet ($J < 0,\ \alpha > 0$) at $T = 0$, we find $A_n = 1/12$ for all $n \neq 0$, as expected for a saturated ferromagnetic ground state. In all other cases, at $T = 0$, we find $A_n \propto 1/n^2$ for large $n$, *i.e.* an algebraic decay of correlations. This may be compared with the exact result [18, p. 160] for the regular Heisenberg antiferromagnet ($J > 0,\ \alpha = 1$), namely $A_n \propto (\ln n)^{1/2}/n$. In this case our theory correctly shows algebraic decay of correlations in the ground state, but under-estimates the strength of short-range correlations.

## 6 Numerical results

For an arbitrary temperature, equations (9), (10), (12), (13), and (14) are solved numerically. We discuss the numerical results in three representative cases. In each case, we give an example of the normal-mode dispersion relations, the spectral weights, and the wave-vector dependent susceptibility (Figs. 1, 3, 5). Owing to our choice of the length scale and the fact that we have two spins per unit cell, the normal modes $\omega_{a,b}$ have a period of $2\pi$ and are symmetric around $q = \pi$, whereas the spectral weights $\mathcal{F}_{a,b}$ and the susceptibility $\chi(q)$ have a period of $4\pi$ and are symmetric around $q = 2\pi$. The temperature dependence of the correlation functions and static susceptibilities for a range of $0 < T < 3J$ appear in Figs. 2, 4, 6. Note, that the correlation functions are multiplied by a factor of 4 in the plots, in accordance with the practice of normalizing the same-site correlation function $A_0 = S(S+1)/3 = 1/4$ to the value of 1, and that $k_B = 1$ in all plots. We only consider cases with $|\alpha| < 1$, as the parameter space $|\alpha| > 1$ can be mapped to $|\alpha| < 1$ by use of the transformation (4).

Common to all temperature-dependent plots (Figs. 2, 4, 6) is the observation that already for $T \geq J$, the correlation functions and the susceptibility agree well with their analytic high-temperature expansions. At low temperatures, one can distinguish clearly between antiferromagnetic correlations showing a maximum at $T \approx 0.3J$ (Fig. 2 and $A_1'$ in Fig. 4), and ferromagnetic correlations reaching their highest values at $T = 0$ (Fig. 6 and $A_1$ in Fig. 4). This feature has already been observed in Ref. [14], and seems to be characteristic to our results. The plots of the normal modes and spectral weights reveal the nature of the local order as expected from the respective signs of $J$ and $\alpha$. These quantities are plotted at temperatures $T \ll |J|$, in order to reveal their structure more clearly. We observe, that varying the temperature on an energy scale of $\alpha J$ has a minor influence on the plotted quantities, *i.e.* the relevant energy scale for the temperature dependence of the observed quantities seems to be the larger of $J$ and $\alpha J$, which in our case is always $J$.

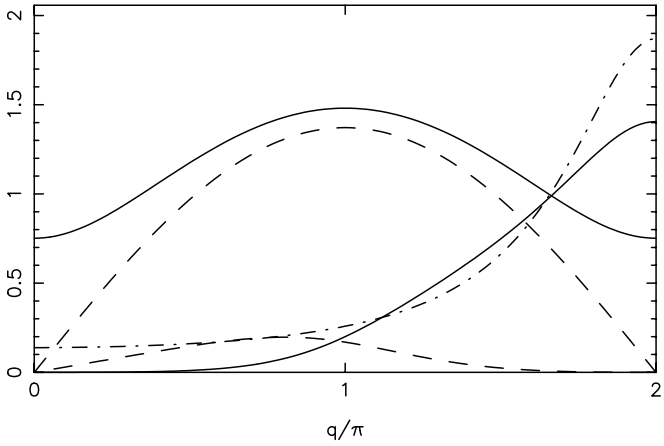


**Fig. 1.** Normal modes $\omega_{a,b}$ (symmetric around $q = \pi$) and respective spectral weights $\mathcal{F}_{a,b}$ for $J = 1$ and $\alpha = 0.9$ at $T \ll |J|$. Solid lines are $\omega_a$ and $\mathcal{F}_a$, dashed lines are $\omega_b$ and $\mathcal{F}_b$. Also given is the wave-vector dependent susceptibility $\chi(q)$ (dash-dotted line) as defined in (18).

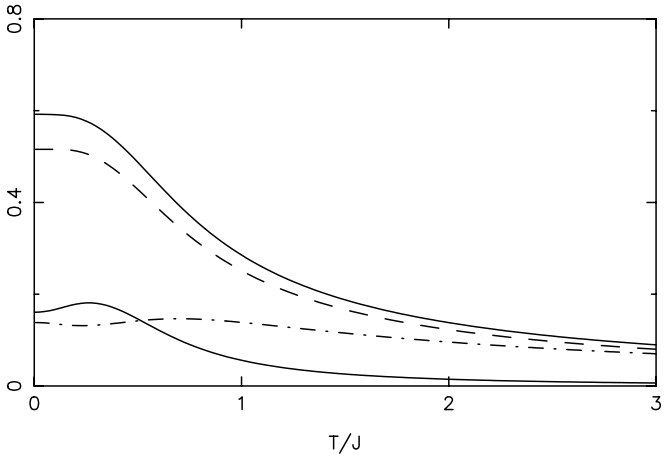


**Fig. 2.** Correlation functions $4|A_1|$ (upper solid line), $4A_2$ (lower solid line), and $4|A_1'|$ (dashed line), and $q = 0$ susceptibility (dash-dotted line) for $J = 1$ and $\alpha = 0.9$.

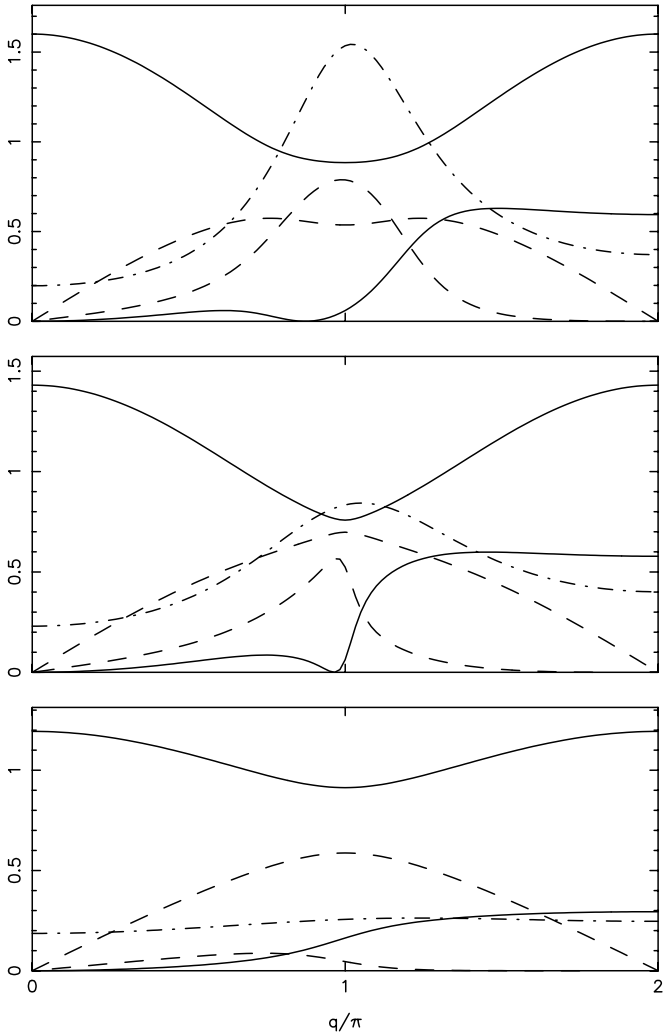


**Fig. 3.** Temperature dependence of the spectrum. Top to bottom: $T = 0$, $T = 0.3J$, $T = J$. Given are normal modes $\omega_{a,b}$ (symmetric around $q = \pi$) and respective spectral weights $\mathcal{F}_{a,b}$ for $J = 1$ and $\alpha = -0.5$. Solid lines are $\omega_a$ and $\mathcal{F}_a$, dashed lines are $\omega_b$ and $\mathcal{F}_b$. Also given is the wave-vector dependent susceptibility $\chi(q)$ (dash-dotted line).

Figs. 1 and 2 refer to the "pure" antiferromagnetic chain, *i.e.*, a chain with $J > 0$ and $\alpha > 0$. From Fig. 1, the behaviour in the limit $\alpha \to 1$ can be seen as the normal modes become degenerate at $q = \pi$ and the spectral weights select the relevant mode for $q < \pi$ and $q > \pi$, respectively. The susceptibility peaks at $q = 2\pi$, *i.e.*, the antiferromagnetic point. The contribution to the scattering at that point comes from the gapped branch $\omega_a$. The approximations made in our theory do not allow the lower branch $\omega_b$ to have a gap at $q = 0$, *i.e.* the lower branch is reminiscent of a Goldstone mode. In consequence, the susceptibility does not decay exponentially at very low temperatures, but remains finite (Fig. 2). The sum of the spectral weights $\mathcal{F}_a + \mathcal{F}_b$, *i.e.* the integrated neutron-scattering intensity, has a finite slope at $q = 0$ and agrees qualitatively with experiments performed at low temperatures [1, Fig. 10]. Looking at Fig. 1, at higher temperatures the displayed quantities are smaller and show less dispersion, and no radical new effects emerge.

The next case (Figs. 3, 4) is a "mixed" chain of antiferromagnetic bonds alternating with ferromagnetic bonds ($J > 0,\ \alpha < 0$). The maximum in the susceptibility $\chi(q)$ at $q = \pi$ and $q = 3\pi$, indicates a locally ordered two-up-two-down spin pattern. Note that the spectral weight for $\omega_b$ vanishes at $q = 0$ and $q = 2\pi$ and mimics the $q$-dependence of $\chi(q)$. In Fig. 3, we have also given representative plots of the spectra for three different temperatures (increasing form top to bottom). With increasing temperature the susceptibility becomes independent of $q$ and approaches its high-temperature value of $\beta/4$ over the whole range of the Brillouin zone.

Finally, a pure ferromagnetic chain ($J < 0,\ \alpha > 0$) is given in Figs. 5 and 6. As expected for a ferromagnetically ordered chain at $T = 0$, the correlation functions $A_1$, $A_1'$,

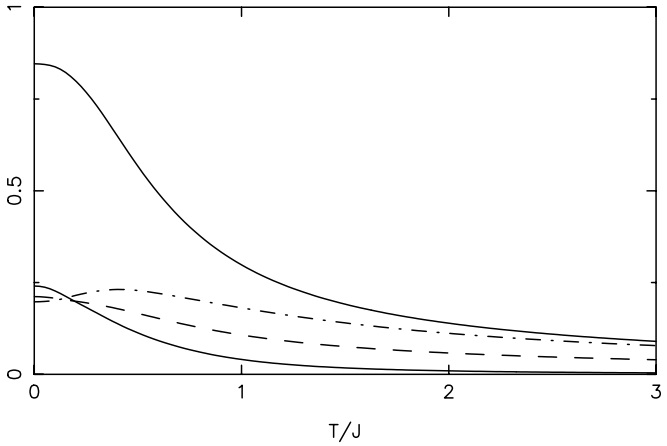


**Fig. 4.** Correlation functions $4|A_1|$ (upper solid line), $4|A_2|$ (lower solid line), and $4A_1'$ (dashed line), and $q = 0$ susceptibility (dash-dotted line) for $J = 1$ and $\alpha = -0.5$.

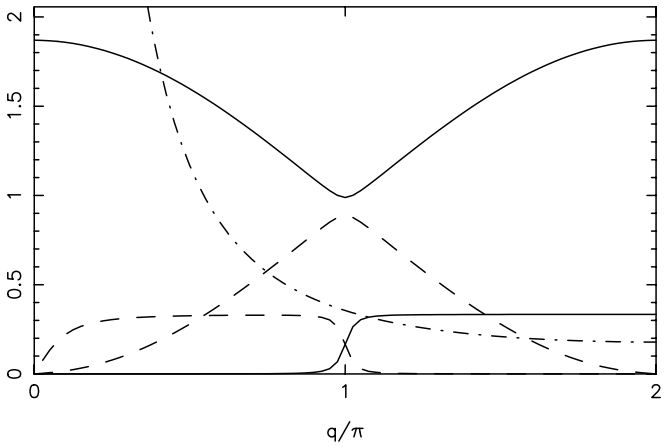


**Fig. 5.** Normal modes $\omega_{a,b}$ (symmetric around $q = \pi$) and respective spectral weights $\mathcal{F}_{a,b}$ for $J = -1$ and $\alpha = 0.9$ at $T \ll |J|$. Solid lines are $\omega_a$ and $\mathcal{F}_a$, dashed lines are $\omega_b$ and $\mathcal{F}_b$. Also given is the wave-vector dependent susceptibility $\chi(q)$ (dash-dotted line).

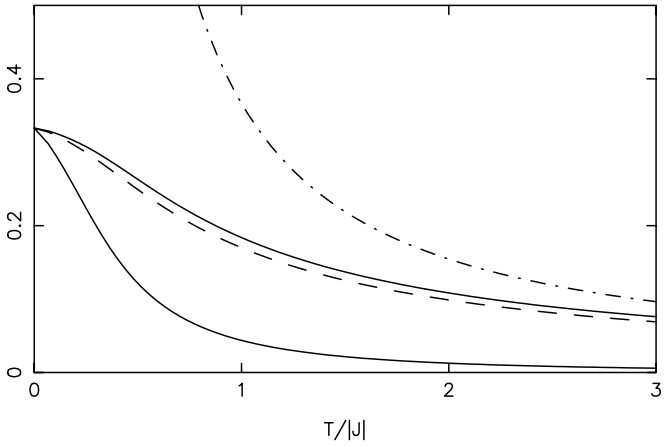


**Fig. 6.** Correlation functions $4A_1$ (upper solid line), $4A_2$ (lower solid line), and $4A_1'$ (dashed line), and $q = 0$ susceptibility (dash-dotted line) for $J = -1$ and $\alpha = 0.9$.

and $A_2$ take the value of $1/12$, irrespective of the coupling constants $J$ and $\alpha$. This result can also be derived analytically from our equations. Consequently, the susceptibility diverges at $q = 0$ for small $T$ as $1/T$.

## 7 Conclusions

Our theoretical approach to the dimerized chain provides useful results for quantities observed in neutron scattering experiments. In addition, we provide a number of analytic expressions for various quantities shown to be correct for certain points in the parameter space of $J$, $\alpha$, and $T$. It must be emphasized, that *a priori* the quality of our theory does not depend on the size and sign of $\alpha$, and we demonstrate it is exact for $\alpha = 0$. We provide expressions for observable quantities like the van Hove response and the susceptibility in terms of the correlation functions $A_1$, $A_1'$, and $A_2$, and the model parameters $J$ and $\alpha$ at arbitrary temperatures, and our theory therefore enables the interpretation of experiments in a straightforward manner.

For the case of an antiferromagnetic chain, in our theory a gapless branch, is always present for any non-zero $\alpha$, although there is no weight in it at the points of high symmetry in the Brillouin zone. We obtain correct results for this case for high temperatures and for $\alpha = 0$. At low temperatures, the decay of correlations with increasing distance compare well with exact results. The integrated neutron-scattering intensity can be fitted to experimental results in order to derive information about the exchange constants $J$ and $\alpha$.

The results given for mixed $S = 1/2$ chains (Fig. 3, 4) cannot easily be compared to experimental data, as no such materials have been studied by neutron scattering techniques yet. However, organic compounds exhibiting alternating antiferromagnetic and ferromagnetic exchange do exist [12], and it may be possible to obtain them in sufficient quality for neutron scattering experiments in the near future. We predict quite striking changes in the van Hove response as the temperature is increased.

For the ferromagnetic chain we believe our excitation spectrum to be accurate over the whole temperature range, as no gap can be expected in this case [10]. Our theory correctly shows a long-range ordered state at $T = 0$. To the best of our knowledge, there are no experiments performed yet on ferromagnetic alternating chains.

Finally, we would like to remark that low-temperature properties of one-dimensional systems are generally difficult to investigate experimentally, as there will always be signatures of higher-dimensional interactions below a finite temperature. Given the increasing number of compounds found by ingenious manufacturing and the progress in experimental skills, one can be confident that many more experimental results on low-dimensional magnetic materials will emerge in the future.

One of us (SWL) worked on the study while a guest of Dr. K. N. Trohidou at the National Centre for Scientific Research, "De-

mokritos", with financial support from the EU through the contract ERBFMB1CT961209.

## References


1. L. P. Reignault, M. Aïn, B. Hennion, G. Dhalenne, and A. Revcolevschi, Phys. Rev. B **53**, 5579 (1996).
2. M. Weiden, R. Hauptmann, C. Geibel, F. Steglich, M. Fischer, P. Lemmens, and G. Güntherodt, Z. Phys. B **103**, 1 (1997).
3. B. Lake, D. A. Tennant, R. A. Cowley, J. D. Axe, and C. K. Chen, J. Phys.: Condens. Matter **8**, 8613 (1996).
4. A. W. Garrett, S. E. Nagler, D. A. Tennant, B. C. Sales, and T. Barnes, Phys. Rev. Lett. **79**, 745 (1997).
5. R. A. Cowley, B. Lake, and D. A. Tennant, J. Phys.: Condens. Matter **8**, L179 (1996).
6. B. Lake, R. A. Cowley, and D. A. Tennant, J. Phys.: Condens. Matter **9**, 10951 (1997).
7. M. Aïn, J. E. Lorenzo, L. P. Reignault, G. Dhalenne, A. Revcolevschi, B. Hennion, and T. Jolicœur, Phys. Rev. Lett. **78**, 1560 (1997).
8. I. Affleck, in *Dynamical Properties of Unconventional Magnetic Systems*, *NATO ASI Series*, edited by A. T. Skjeltorp and D. Sherrington (Kluwer, Dordrecht, 1998), in press.
9. R. A. Cowley, in *Dynamical Properties of Unconventional Magnetic Systems*, *NATO ASI Series*, edited by A. T. Skjeltorp and D. Sherrington (Kluwer, Dordrecht, 1998), in press.
10. J. C. Bonner and H. W. J. Blöte, Phys. Rev. B **25**, 6959 (1982).
11. H. Manaka, I. Yamada, and K. Yamaguchi, J. Phys. Soc. Japan **66**, 564 (1997).
12. M. Hagiwara, Y. Narumi, K. Kindo, T. Kobayashi, H. Yamakage, K. Amaya, and G. Schumauch, J. Phys. Soc. Japan **66**, 1792 (1997).
13. K. Hida, J. Phys. Soc. Japan **63**, 2514 (1994).
14. J. Kondo and K. Yamaji, Prog. Theoret. Phys. **47**, 807 (1972).
15. S. W. Lovesey, *Condensed Matter Physics: Dynamic Correlations*, 2nd ed. (The Benjamin/Cummings Publishing Co., Menlo Park, 1986).
16. P. M. Richards, Phys. Rev. Lett. **27**, 1800 (1971).
17. S. A. Scales and H. A. Gersch, Phys. Rev. Lett. **28**, 917 (1972).
18. A. Auerbach, *Interacting Electrons and Quantum Magnetism* (Springer-Verlag, New York, 1994).